



# Performance Enhancement of Centrifugal Compressor with Addition of Splitter Blade Close to Pressure Surface

A. Malik<sup>†</sup>, Q. Zheng, A. A. Zaidi and H. Fawzy

*College of Power and Energy Engineering, Harbin Engineering University, Harbin 150001, China*

<sup>†</sup>*Corresponding Author Email: [adilmalik@hrbeu.edu.cn](mailto:adilmalik@hrbeu.edu.cn)*

(Received December 4, 2017; accepted April 3, 2018)

## ABSTRACT

This paper exemplified a way to increase pressure ratio and improve efficiency with addition of multi splitters in centrifugal impeller with a vaneless diffuser. DDA 404-III back swept impeller of centrifugal compressor, studied through experiment is modified with the addition of splitters blades and a sample impeller is designed and analyzed with big splitter close to pressure surface and small splitter close to suction surface. Keeping all flow conditions and impeller definitions, same as experimentally validated impeller, in order to investigate effects of the location of the splitters between two main blades. It was observed that total pressure ratio is increased from 4.1 to 4.5 with 2 % increase in efficiency with big splitter close to pressure surface of main blade and small splitter close to suction surface of main blade. It was observed that relative Mach number reduces at inlet of modified impeller.

**Keywords:** Numerical simulation; Multi splitter blades; DDA 404-III Impeller; Centrifugal Compressor

## 1. INTRODUCTION

The centrifugal compressors are widely used in aerospace, oil and gas, automobile, air separation and other industry [D. Japikse \(1996\)](#), [Li et al. \(2015\)](#). Centrifugal compressor design is restricted by the inlet Mach number limitations and blade loading i.e. pressure differences between impeller blade suction and pressure side. In case the pressure difference is higher than a certain value, the fluid flow stream separates from the suction surface at that location and generate more losses in the radial impeller. The blade pressure loading increases from leading edge to trailing edge of the impeller. Therefore, flow-separation is easy to take place near the exit of the impeller. This flow pattern at the exit of the compressors is well known and often named as the "jet-wake" flow [D. Japikse \(1996\)](#). An arrangement of shorter length blades, called "1/2 blades" or "splitter blades" are designed in passages between the two full-length blades in order to reduce the separation in impeller. In a passage between splitter blade and the full blade a set of the splitter blade was introduced symmetrically in the mid of the channel. There are very limited studies to address the splitter location affecting the compressor performance.

Centrifugal compressor designers use the splitter to achieve the high-pressure ratio and avoid the choking of the flow in the throat of the leading edge of the main blade of radial impellers [Xu et al. \(2012\)](#)

[a,b](#)). The conventional design approach for the splitter is to design the same blade profile on the full and splitter blades, with the splitter blade placed at mid-pitch of the two main blades. Studies on the introduction of splitter vanes in the impeller passage have been conducted in the past. [Fardian \(1987\)](#), [Millour \(1988\)](#), [Teipel and Wiedermann \(1988\)](#), [Teipel and Wiedermann \(1987\)](#), [Zangeneh \(1998\)](#). [Fradin \(1987\)](#) did a broad arrangement of investigations on the transonic stream of two centrifugal rotors: one without splitters, and other with it. The arrangement of splitters is similar to main blades and location was at the center amid two main blades. The studies show that flow field at the impeller outlet turned out to be more consistent once the splitters were utilized. The splitter compressor have better performance than the one without the splitter. [Millour \(1988\)](#) examined the same configuration by using a three-dimensional flow analysis. It was demonstrated that the splitters main impact is to lessen loading on impeller blades, and also to diminish the jet/wake impact at the impeller trailing edges.

In recent years a lot of research is in progress to increase the pressure ratio, changes in experimental strategies and 3D numerical simulation with CFD accelerated these investigations. A lot of work has been done in identifying unknown losses in radial compressor aerothermodynamics and estimating numerous fluid flow characteristics [Larosiliere and Skoch \(1997\)](#), [McKain and Holbrook \(1982\)](#). The

numerical method with Computational Fluid Dynamics (CFD) has been widely used in different aerodynamic studies and designs Zangeneh (1998), Xu *et al.* (2004, 2009 a,b, and 2010), Hattori (2017). CFD can be a tool to do whole compressor stage analyses and optimize the centrifugal compressor performance during the design process. Kim *et al.* (2012), Roytta *et al.* (2009), Xu *et al.* (2008 and 2009 b,c). Definite estimations of the internal fluid flow field made by Dean (1971), Kano *et al.* (1982), Moore *et al.* (1984), Vavra (1970), Krain (1981), Hathaway *et al.* (1993), Skoch *et al.* (1997) are extremely helpful in filling holes of unknown phenomena of fluid flow in compressors. Additionally, use of CFD linked with these benchmarks experimental information can extraordinarily increase the researcher's knowledges and improve our capacity to analyze optimum design options.

The Jet-Wake flow pattern in centrifugal impeller was additionally seen by many researchers Chriss *et al.* (1996), Eckardt (1988), Abramian and Howard (1994), Eckardt (1976), Carey and Fraser (1993), Farge and Johnson (1992), Joolyn (1991), Fagan and Fleet (1991). Particularly, by Eckardt (1976) with Laser-2-Focus estimation systems, described such a flow pattern in detail. Tamaki *et al.* (1998) utilized splitter blade with different camber angle at inducer than the main blade in design of a radial impeller having 4.3 pressure ratio. He achieved enhanced blade loading distribution and efficiency. By changing the blade thickness distribution and blade shape, Ona *et al.* (2002) renovated the compressor and succeed in reducing the rapid acceleration and deceleration of fluid flow at leading edge and separation phenomena at hub.

The splitter compressor has better performance than the one without the splitter. Number of researchers have studied the effect of splitters in pairs, however, no one has studied the effect of double splitter with different sizes. Therefore, in order to fill this gap, in this Research, DDA 404-III back swept impeller studied through experiment by Mckain and Holbrook and analyzed through CFD code ADPAC program by L. M Larosiliere, Skoch, Prahst is modified and a sample impeller is designed with small splitter close to suction surface and big splitter close to pressure surface. In this study, the splitters were designed with the same blade profile as main blades, with addition of multi splitters in centrifugal impeller with a vaneless diffuser in order to investigate effects of the location of the splitter between two main blades. Keeping all flow conditions tip diameter, mass flow, rotational speed, theta definition of main and splitter blades, backswept definition at trailing edge and thickness definition, same as experimentally validated impeller. Studies in this paper show that the splitter position affects the centrifugal compressor performance with increase in pressure ratio and improvement in efficiency.

## 2. VALIDATION OF NUMERICAL SIMULATION

For validation of code and procedure of simulation, high pressure ratio DDA 404-III back swept

impeller studied through experiment by Mckain and Holbrook and analyzed through CFD code ADPAC program by L. M Larosiliere, Skoch and Prahst was analyzed. The impeller definition is enumerated below in Table 1:

**Table 1 Impeller definition**

S.No.	Parameter	value
1.	Pressure ratio	4
2.	Mass flow	4.54 kg/sec
3.	RPM	21789
4.	Specific speed	0.60
5.	Impeller tip speed	492 m/sec
6.	No. of main blades	15
7.	No. of splitter blades	15
8.	Impeller exit diameter	0.431m
9.	Tip clearance at trailing Edge	0.000203m
10.	Tip clearance at leading edge	0.0001524m
11.	Backswept from radial	50 degree

The pictorial view of original impeller and monitoring points are shown in Fig. 1. McKain and Holbrook (1982) has given the blade coordinates, details of aerodynamic design and mechanical specifications.

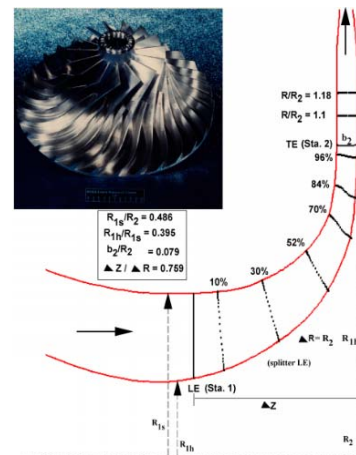


**Fig. 1. Original impeller sketch with monitoring points.**

## 3. COMPUTATIONAL METHOD

The computational simulation of experimental impeller was performed using Ansys CFX. The blade geometry as narrated by McKain and Holbrook (1982) is used to make the model in Ansys Blade Gen. Figure 2 shows 3-D model and meridional view. Figure 3 shows blade to blade view of impeller in Ansys Blade Gen. The computational model is a bit different from original impeller. In original impeller the splitter blade profile and thickness are a bit different from main blade. But due to restriction of software splitters was modeled with same profile and thickness definition as per main blade in computational model.

The model is exported to Ansys Turbo Grid for meshing. A fine mesh is generated with total number of nodes 1084655 and Total Number of

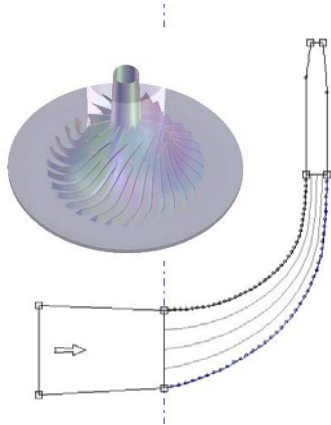


**Fig. 2. 3-D model and Meridional view of impeller.**

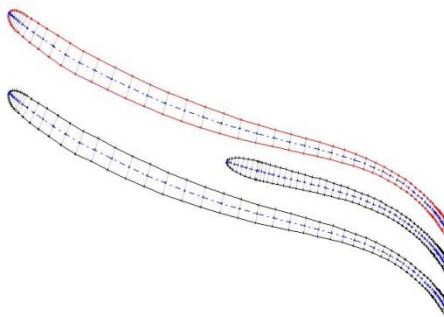


**Fig. 3. Blade to blade view of impeller.**

Elements 1027008 and Number of Hexahedrons 1027008. Figure 4 shows inlet mesh and Fig. 5 shows the mesh at shroud including tip clearance. The computational clearance gap is a bit different from that of measured in experiment. In experiment the shroud clearance was 0.1524 mm at leading edge, 0.61 mm at mid-stream and 0.203 mm at trailing edge of impeller. It is set at 0.1524 mm at leading edge of impeller and 0.203 mm at trailing Edge. It might be diverse at mid span from measured clearance. Keeping in mind the end goal to restrict reversal of flow at the outlet, the outlet boundary of the vaneless diffuser is a bit contracted.

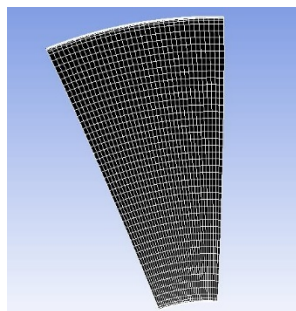


**Fig. 4. Inlet mesh.**

After meshing model is exported to Ansys CFX Pre. The experimental total pressure at the inlet boundary is specified along with temperature. The direction of flow is set at zero swirl angle. Mass flow 4.54 kg/sec is given at the outlet boundary of the computational domain. The solution results are obtained by solving the 3D steady compressible Reynolds-averaged Navier–Stokes equations and a

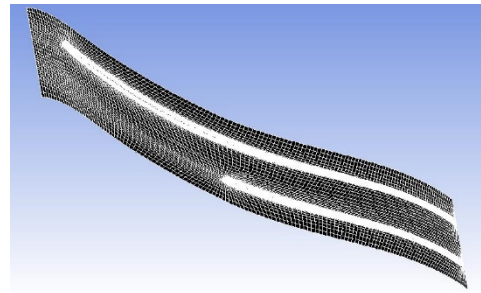


**Fig. 5. Mesh at shroud including tip clearance.**

finite-volume method is used to discretize the equations. k-epsilon turbulence model is used. Air is treated as ideal gas.

To eliminate the effect of grid size on the numerical simulation, the investigation of a grid-independence is performed on the impeller. Five models are computed under the same inlet pressure and temperature and outlet mass flowrate conditions with variation in number of grid points. It was observed that from 0.8 million to 0.9 million grid points, changes in efficiency becomes negligible. As shown in Fig. 6. Resultantly, total number of grid points of the impeller was set at approximately 1 million.

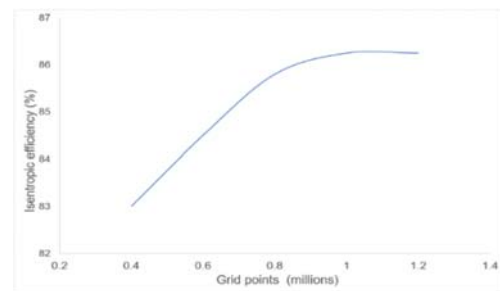


**Fig 6. Numerical results with different grid points.**

#### 4. OVERALL PERFORMANCE

The overall performance of radial impeller with vaneless diffuser at a radius ratio of 1.18 computed through numerical simulation is shown in Figs. 7 & 8 with experiment results and results computed by Prahst and Scotch. Pressure ratio predicted by numerical simulation through Ansys CFX is quite close to experiment and computed by Prahst and Scotch. Ansys CFX computed efficiency is 86.25%, which is 0.5% lower than measured efficiency at a design mass flow rate of 4.54 kg/sec and total to total pressure ratio of 4.1. The performance curves are also computed and found close to experimental results. The circumferentially averaged static pressure distributions at design flow rate was numerically computed as shown in Fig. 9. The experimental measurements show pressure distribution along the shroud while the calculations show simple basic area-average of the CFD results. Computed results are quite close to measured static pressure distribution, however, close to the impeller leading edge numerical simulation demonstrates the impact of leading edge better than measurements in experiments.

The experimental measurements and numerically simulated spanwise distributions of circumferentially-average total pressure at a radius ratio of 1.18 computed by author and measured through experiment and computed by Prahst and Scotch is shown in Fig. 10. Again, a good match observed between computed and measured data. The generation of entropy in Fig. 11 to 16 is predicted by Prahst and Scotch in their computational analysis, it is compared with the results computed by Ansys CFX, which shows quite good match. At 10% chord once flow enters in impeller, the elevated entropy area is very less and observed only close to solid surfaces i.e. blade and hub surfaces. At 30 % chord it is observed that elevated entropy area is starting to accumulate with the shroud, likewise in hub wall too. Continuing toward 52 %, at mid-stream more accumulation of two elevated entropy centers can be seen close to the shroud. It is prudent to highlight that the most noteworthy entropy area is positioned close to junction of tip clearance and at main blade pressure side. Consequently, moving toward the trailing edge at 70% and 96% chord, the elevated entropy close to the tip display a quick diffusion toward the center of conduits. At entrance to vaneless diffuser or at 1.01 radius ratio, elevated entropy areas are seen close to the splitter and main blade impeller trailing edges. Thick blade trailing edges add to dump loss. Likewise, the fast blending amongst elevated and sunken entropy areas was noted while moving toward vaneless diffuser to higher radius ratios.

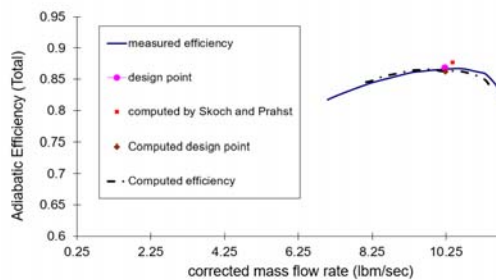


Fig. 7. Efficiency at radius ratio of 1.18.

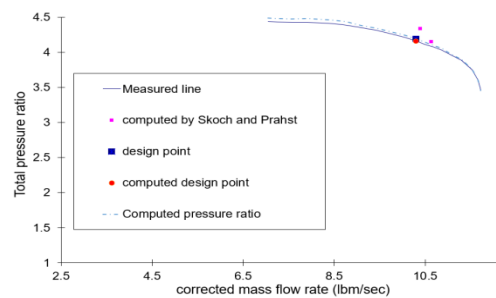


Fig. 8. Total Pressure ratio at radius ratio of 1.18.

### 5. MODIFICATION OF MULTI SPLITTER BLADE

Above mention impeller was modified by adding multi splitters in order to analyze its effect on fluid flow in impeller passages and its effect on overall performance. The impeller was modified by keeping tip diameter, mass flow, rpm, theta and

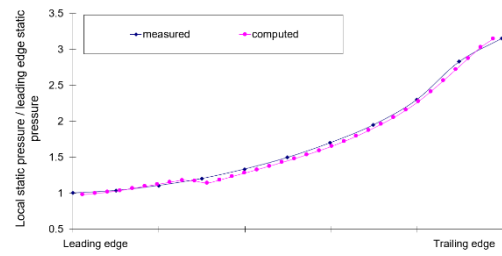


Fig. 9. Circumferentially averaged static pressure distributions.

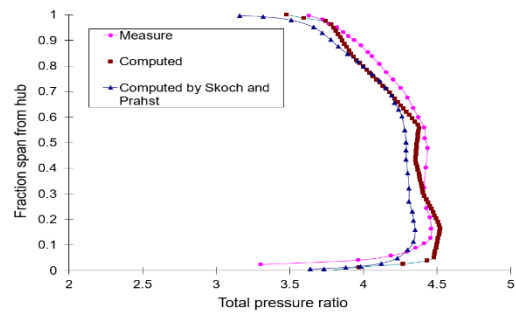


Fig. 10. Spanwise distributions of circumferentially-average total pressure at a radius ratio of 1.18.

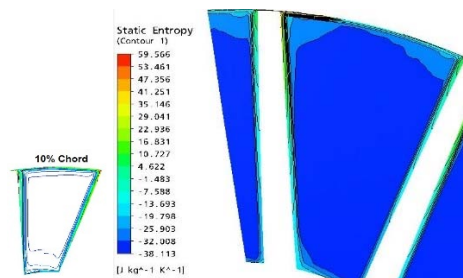


Fig. 11. Entropy distribution at 10% chord.

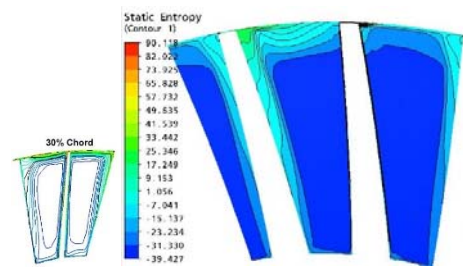


Fig. 12. Entropy distribution at 30% chord.

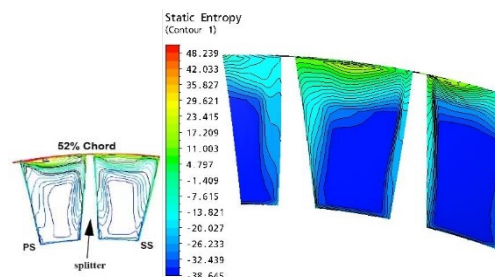


Fig. 13. Entropy distribution at 52% chord.

backswep definition and thickness definition same as original that is constant. Impeller was modified with respect to big splitter and small splitters position too in order to observe its effect on the flow field.

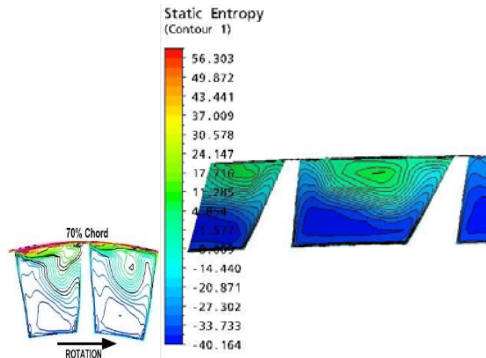


Fig. 14. Entropy distribution at 70% chord.

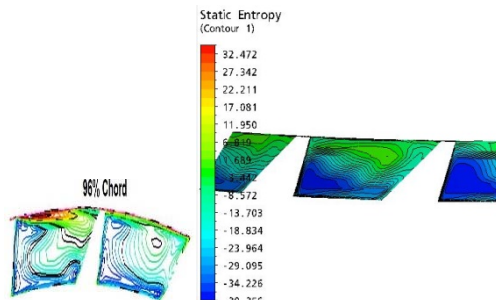


Fig. 15. Entropy distribution at 96% chord.

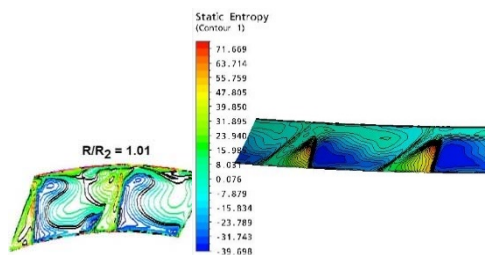


Fig. 16. Entropy distribution at radius ratio 1.01.

The original impeller was designed with 15 full blades and 15 splitter blades. It was modified to 11 main blades, 11 small splitter blades and 11 big splitter blades by keeping theta, backswept and thickness definition as per original. Impeller was design with respect to position of splitters and position of first and second splitter in normalized meridional length. Numerous positions of splitters were analyzed in order to get maximum total pressure at constant flow rate and to achieve higher efficiency. The position mentioned in Table 2 and 3 were selected after number of hit and trial simulations.

**Table 2 Position of big and small splitter (spanwise from suction surface)**

	Small splitter	Big splitter
Modified impeller	30%	60%

**Table 3 Position of big and small splitter (normalized meridional length)**

	m/m <sub>2</sub>	Modified impeller
Big splitter	hub	35%
	shroud	37%
Small splitter	hub	20%
	shroud	22%

The modified impeller was analyzed with Ansys CFX, as per procedure of computation of original impeller. Figures 17 and 18 show different views of modified impeller.

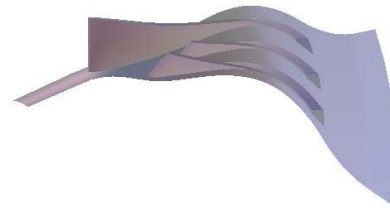


Fig. 17. 3D view of modified impeller.

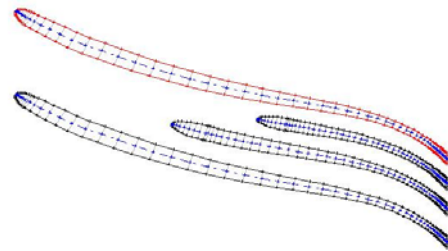
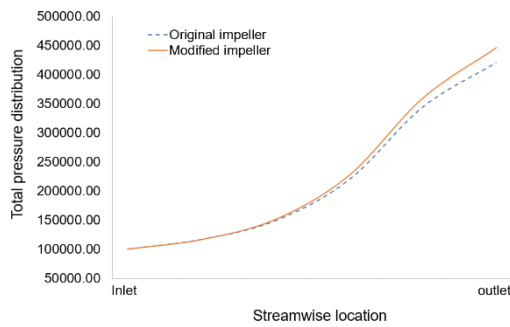


Fig. 18. Blade to blade view of modified impeller.

## 6. EVALUATION OF MODIFIED IMPELLER

Several CFD calculations showed that the increase in the number of blades did not contribute to the increase in pressure ratio but deteriorated efficiency. A narrowed blade passage, which increases wetted area and accelerates the flow in the impeller cause increase in friction loss. Consequently, it was decided to employ a multi splitter blades which could realize to reduce the Mach number at inducer with better efficiency. Aim is to compress the gas sequentially till higher pressure, beating the limitation of increase in inlet Mach number. Consequently, it was observed that with the modification of big and small splitter blade, total pressure ratio is increased from 4.1 to 4.5 with 2% increase in efficiency. The streamwise distribution of circumferential average total pressure computed in original and modified impeller is shown in Fig. 19. At the leading edges original impeller has 15 blades and modified impeller has 11 blades, therefore, pressure increase is more in original impeller. However, after 20% streamwise location the effect of first splitter and then at 28% streamwise location, effect of second splitter increases the pressure in modified impeller. Which lead to higher pressure ratio at the trailing edge. However, the relative Mach number at leading edges of the compressor is reduced with the lesser number of main blades.

Contour of relative Mach number at 50% Span in original impeller and modified impeller is shown in Figs. 20 and 21. In modified impeller, relative Mach number observed lower then original impeller at inlet of impeller. It was observed that positioning of big splitter close to pressure surface would increase the flow velocity at region near the leading edge of big splitter at the passage between big splitter and main blade. For this reason, there is minor increase in vortex near trailing edge close to the shroud at



**Fig 19. Stream wise distributions of circumferential average total pressure.**

downstream of passage. With the addition of splitters separation has decreased at all of the regions. The splitter position has a high impact near the leading edge area compared to other locations. Relative velocity observed lower than the original impeller at leading edge span wise plot of relative velocity as shown in Fig. 10. In original impeller, the higher relative Mach number is observed due to the splitter leading edge is limiting the flow between splitter blade and pressure side of the blade however in modified impeller due to less separation same phenomena do not exist and fluid flows without any separation due to lesser number of full blades as effect of leading edge disturbance do not effect it. However minor choking due to placement of big splitter near pressure surface of main blade was observed. The throat area differences on both sides of the main blades with multi splitter and single splitter is different. Actually, the high value zone of the total pressure is higher in modified impeller when compared to original impeller. This shows higher efficiency.

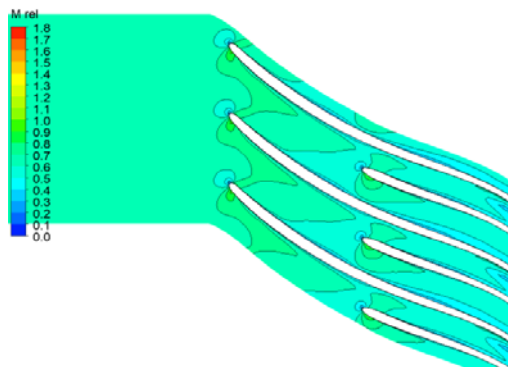


**Fig. 20. Original blade Contour of M rel at 50% Span.**

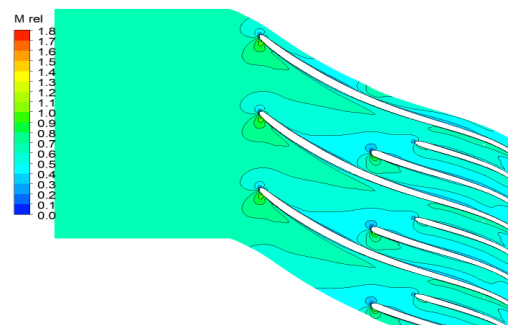


**Fig. 21. Modified blade Contour of M rel at 50% Span.**

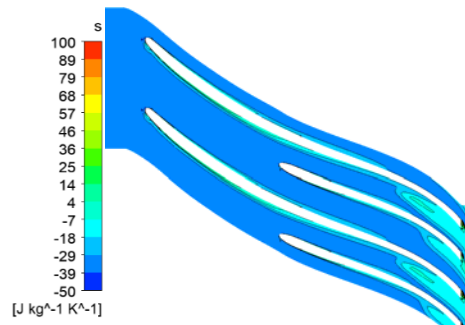


**Fig. 22. Original blade Contour of Entropy at 50% Span.**

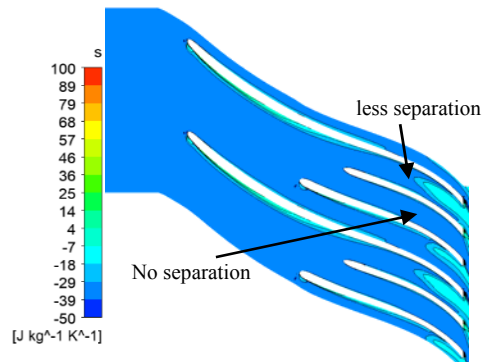


**Fig. 23. Modified blade Contour of Entropy at 50% Span.**

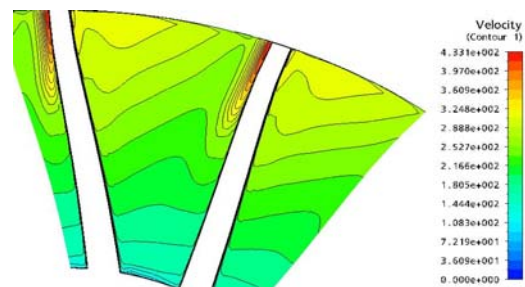


**Fig. 24. Relative velocity at original impeller's Leading edge.**

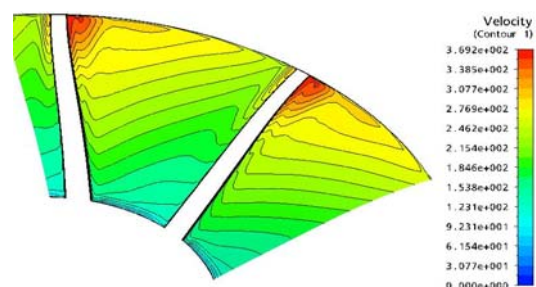


**Fig. 25. Relative velocity at modified impeller's Leading edge.**

Due to modification of splitter blades friction losses due to higher velocity gradient in original impeller has been reduced as the velocity and Mach number on blade surfaces have been reduced in modified impeller as shown in 50% span entropy contour in Figs. 22 and 23. Additionally, losses due to friction have been reduced due lesser number of full blades. The tip leakage flow is reduced which lead to reduction in separation near trailing edges. Losses originated due to tip leakages have been reduced due to lesser number of main blades. The splitter

locations have a higher impact near the leading edge are compared to other sectors. This effect is visible in Figs. 24 and 25 as the relative velocity at modified impeller leading edge shows lower velocities. This feature is because the splitter location changes the blockage of the downstream in all sides of impeller channels. Contour of ratio of meridional velocity and tip speed and M rel at trailing edge is shown in Figs. 26 to 29 respectively. A quite less Mach number observed in a passage between big splitter and small splitter in modified impeller due to choking at inlet of said passage and vortex creation. A uniform flow pattern observed in passage between small splitter and main blade and big splitter and small splitter with reduced separation if we compare it with original impeller. Figures of trailing edges shows the flow patterns of typical Jet and wake flow in both the impellers. It is shown that the wake core for both the impeller is located near the splitter pressure side and also close to shroud side. The core effect looks to move from pressure side to middle of the channel or suction side between main blade and big splitter blade. The wake zones are smaller near shroud and trailing edges due to lesser separation in the presence of splitter blades.

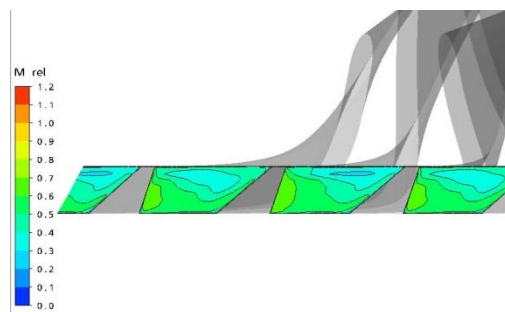


**Fig. 26. Original blade Contour of M rel at trailing edge.**

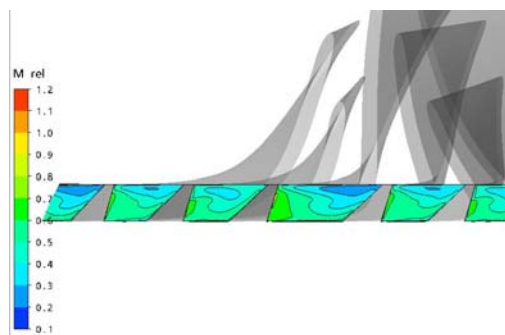


**Fig. 27. Modified blade Contour of M rel at trailing edge.**

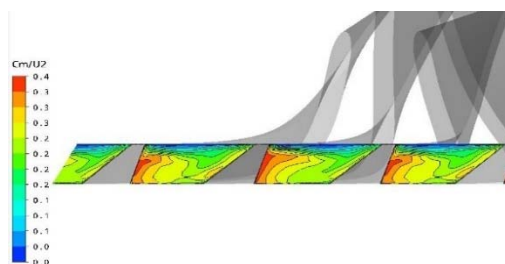


**Fig. 28. Original blade Contour of ratio of meridional velocity and tip speed at trailing edge.**

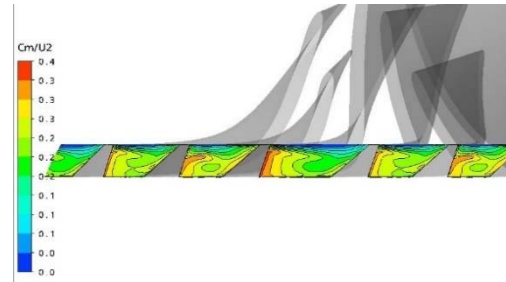


**Fig. 29. Modified blade Contour of ratio of meridional velocity and tip speed at trailing edge.**

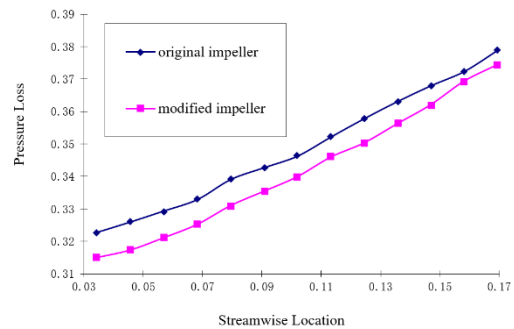


**Fig. 30. Pressure loss in impeller.**

The pressure loss is defined as:

$$\text{Pressure loss} = \frac{P_t - P}{0.5 \rho W_{inlet}^2}$$

Where  $P_t$  is mass average total pressure,  $\rho$  is the mass average density at inlet and  $W$  is the mass average relative velocity at inlet. Pressure loss in original impeller and modified impeller is compared. Figure 30 shows the average pressure loss in original impeller and modified impeller at streamwise locations. It was observed the modified impeller has less pressure loss than original impeller. The same is shown in contour of pressure loss in original and modified impeller at suction surface and pressure surface in Figs. 31 to 34. In pressure surface contour the pressure loss due to placement of big splitter close to pressure surface is visible. Higher pressure loss observed at leading edge of big splitter. Still its lower than pressure loss observed at the original impeller leading edge. Pressure losses near leading edge observed lower in modified impeller. Figures 35 to 38 show pressure loss contours at leading edge and 10% span in original and modified impeller. Pressure loss at leading edge and 10% span contour shows remarkable decrease in loss near pressure surface except near the big splitter leading edge. Near hub section, the low total pressure zone is smaller for the modified impeller. Overall pressure loss in modified impeller was observed lower than original impeller. This may be due to reduction in velocity at inlet and impeller passages. Friction Losses due to higher velocity gradient in original impeller has been reduced as the velocity and Mach number on blade surfaces have been reduced in modified impeller. Due to the deceleration of flow compared to original impeller, flow in the channel is more uniform. In addition, once the circumferential width of the channel of the flow path is reduced due to the presence of splitter blades, the speed difference

caused by the Coriolis force is also reduced. This increases the flow velocity along the radial direction. The same may lead to increase in total pressure at outlet and increase efficiency.

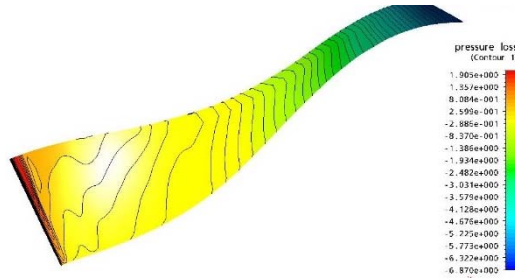


Fig. 31. Pressure loss at original impeller's main blade suction surface.

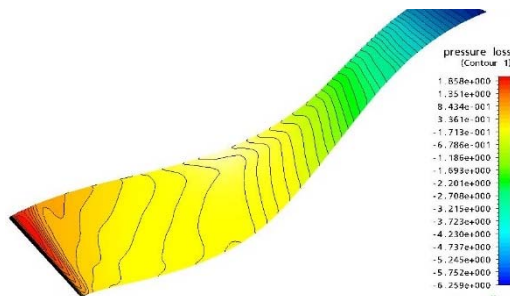


Fig. 32. Pressure loss at modified impeller's main blade suction surface.

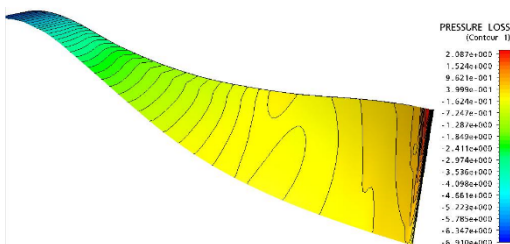


Fig. 33. Pressure loss at original impeller's main blade pressure surface.

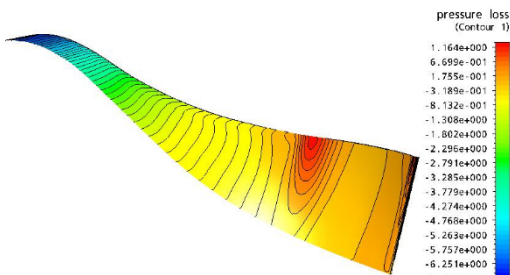


Fig. 34. Pressure loss at modified impeller's main blade pressure surface.

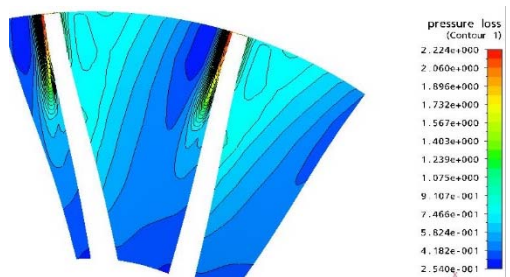


Fig. 35. Pressure loss at original impeller's Leading edge.

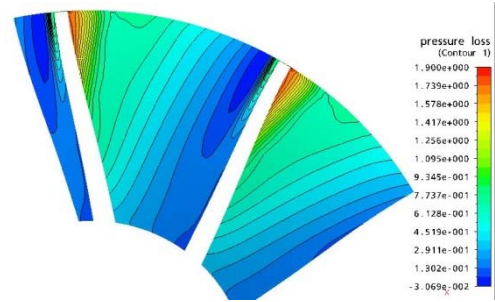


Fig. 36. Pressure loss at modified impeller's Leading edge.

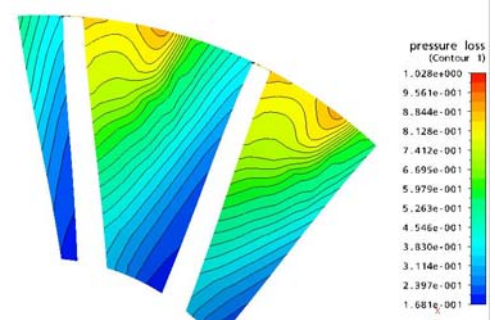


Fig. 37. Pressure loss at original impeller's 10% span.

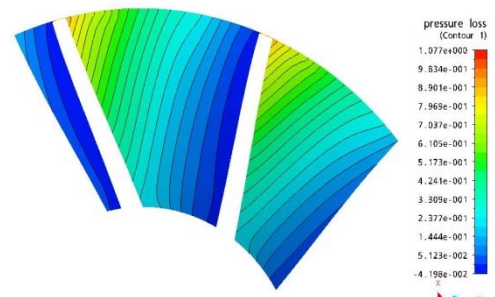
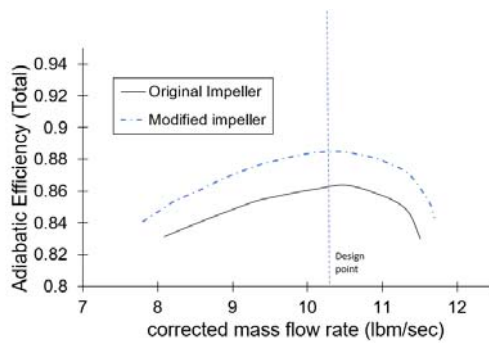


Fig. 38. Pressure loss at modified impeller's 10% span.

A significant performance improvement has been observed in modified impeller. It not only reduces the elevated entropy area, but also generate more uniform fluid flow condition at impeller inlet and exit. The uniform flow will benefit the downstream components of the compressor. The smaller low total pressure zone also indicates that impeller loss is lower and impeller efficiency is high. The flow field distributions agree with the overall efficiency. The shroud low total pressure zone is lower in modified impeller. This trend indicates that the modified impeller has uniform flow fields and produces the less mixing loss at downstream. Therefore, it has better impeller efficiency, which also benefits the overall efficiency. The placement of splitters is more efficient than full blades and the static pressure increase mainly happens when flow exist both splitters and main blade exist. Performance curves of modified impeller at various mass flowrate is shown in Figs. 39 and 40.

## 7. CONCLUSION

It is concluded that splitter blades have positive impacts on the compressor impeller performance



**Fig. 39. Efficiency at radius ratio of 1.18.**

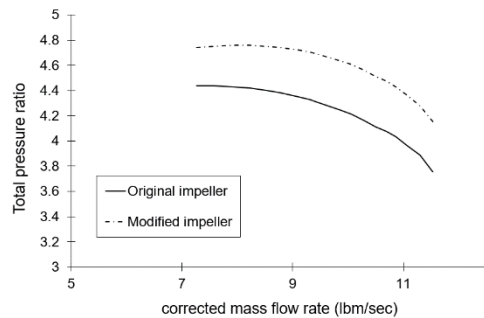


**Fig. 40. Total Pressure ratio at radius ratio of 1.18.**

once gas is compressed systematically with the alteration in location of splitters i.e. big or small splitters in cascade. The placement of splitters is more efficient than full blades. Overall pressure loss in modified impeller was observed lower than the original impeller. Total pressure ratio is increased from 4.1 to 4.5 with 2% increase in efficiency with placement of big splitter close to pressure surface of main blade and small splitter close to suction surface of main blade due to reduction in relative velocity and Mach number. In modified impeller flow is more uniform and friction losses have been reduced. In addition, once the circumferential width of the channel of the flow path is reduced due to the presence of splitter blades, the speed difference caused by the Coriolis force is also reduced. This increases the flow velocity along the radial direction and on the pressure side of the main blade. The same may lead to increase in total pressure at outlet.

## REFERENCES

- Abramian, M. and J. H. G. Howard (1994). Experimental Investigation of the Steady and Unsteady Relative Flow in a Model Centrifugal Impeller Passage. *Journal of Turbomachinery* 116, 269 - 279
- Carey, C. and Fraser, S. M. (1993), *Studies of the Flow of Air in a Model Mixed Flow Pump by Laser Doppler Anemometry, Part 2: Velocity Measurements within the Impeller*. NEL Report No. 699.
- Chriss, R. M., Hathaway M. D., and Wood, J. R. (1996), Experimental and Computational Results from the NASA Lewis Low-Speed Centrifugal Impeller at Design and Part-Load Conditions. *Journal of Turbomachinery*, 118(1), 55-65.
- Cumpsty, N. A., (1989), *Compressor Aerodynamics*, Longman Scientific and Technical, Essex, England, ISBN 0-582-01364-X
- Dean, R., (1971), On the Unresolved Fluid Dynamics of the Centrifugal Compressor, *Advanced Centrifugal Compressors*, ASME Publications.
- Eckardt, D. E. (1976). Detailed Flow Investigations with a High-Speed Centrifugal Compressor Impeller. *Journal of Fluids Engineering, Trans. of ASME*, 98, 390-402.
- Fagan, J. R. and Fleet, S. (1991), Impeller Flow Field Measurement and Analyses. *Journal of Turbomachinery*, 113(4), 670-679.
- Farge, T. Z. and Johnson M. W. (1992), Effect of Flow Rate on Loss Mechanisms in a Backswept Centrifugal Impeller. *Int. Journal of Heat and Fluid Flow*, 13, 189- 195.
- Fradin, C., (1987), *Inverstigation of the Three-Dimensional Flow near the Exit of Two Backswept Transonic Centrifugal Impellers*, Proc. of the Eighth International Symposium in Air Breathing Engines, 149 – 155.
- Hathaway M. J., R. M. Chriss, J. R. Wood and A. J. Strazisar (1993), Experimental and Computational Investigation of the NASA Low-Speed Centrifugal Compressor Flow Field, *ASME J. of Turbomachinery*, 115, 527-542.
- Hattori, H., T. Houra, A. Kono and S. Yoshikawa, (2017). Computational Fluid Dynamics Study for Improvement of Prediction of Various Thermally Stratified Turbulent Boundary Layers, *J. Energy Resour. Technol.* 139 (5).
- Japikse, D. (1996), *Centrifugal Compressor Design and Performance*, Concepts ETI, Inc.
- Joolyn, H. D. (1991), Centrifugal Impeller -- Aerodynamics, An Experimental Investigation. *Journal of Turbomachinery*, 113(4), 660-669.
- Kano, F., Tazawa N. and Fukao Y. (1982) *Aerodynamic Performance of Large Centrifugal Compressors*, ASME Paper 82-GT-17.
- Kim, S. , J. Park, and J. Baek, (2012), *A numerical study of the effects of blade angle distribution on the performance and loss generation of centrifugal compressor impellers*, Proceedings of the Institution of Mechanical Engineers Part A- Journal of Power and Energy, 2226(A2), 208-217.
- Krain, H. (1981). A Study on Centrifugal Impeller and Diffuser Flow, *Transactions of the ASME*, 103, 688-697.
- Krain, H. Swirling (1988). Impeller Flow. *Journal of Turbomachinery*, ASME, 110(2), 122-128.
- Larosiliere, L. M. and G. J. Skoch (1997), *Aerodynamics synthesis of a centrifugal*

- impeller using CFD and measurements*, by U.S. Army Research Laboratory NASA Lewis Research Center NASA Technical Memorandum 107515 AIAA-97-2878.
- Li, Y., T. Lige, Zhang A., Xie Y., B. Jian Shen; H. Li; W. Li, L. Shiqi (2015), Energy Analysis for Air Separation Process Under Off-Design Conditions, *J. Energy Resour. Technol.*; 137 (4).
- McKain, T. F. and G. J. Holbrook (1982), *Coordinates for a High Performance 4:1 Pressure Ratio Centrifugal Compressor*, NASA Contract NAS 3-23268, (to be published as a NASA CR)
- Millour, V., (1988), *3D Flow Computations in a Centrifugal Compressor with Splitter blade Including Viscous Effect Simulation*, 16<sup>th</sup> Congress, International Council for Aeronautical Societies, 1, 842-847.
- Moore, J., J. G. Moore and P. H. Timmis (1984), Performance Evaluation of Centrifugal Compressor Impellers Using Three-Dimensional Viscous Flow Calculations, *J. of Engineering for Gas Turbines and Power*, 106, 475-481.
- Ona, M., H. Kawamoto and Y. Yamamoto, (2002), Approach to High Performance Transonic Centrifugal Compressor, *AIAA* 2002-3536.
- Roytta, P., A. Gronman, A. Jaantinen, T. Turunen-Saaresti, and J. Backman, (2009), Effects of different blade angle distribution on centrifugal compressor performance, *International Journal of Rotating Machinery*, Article ID 537802, 1-9.
- Skoch G. J., Prahst P. S., Wernet M. P., Wood J. R. and Strazisar A. J., (1997), *Laser Anemometer Measurements of The Flow Field in a 4:1 Pressure Ratio Centrifugal Impeller*, ASME Paper 97-GT-342.
- Tamaki, H., Yamaguchi, S., Nakao, H., Yamaguchi, H., Ishida, K. and Mitsubori, K. (1998), *Development of Compressor for High-Pressure Ratio Turbocharger*, IMechE C554/002.
- Teipel I. and Wiedermann, A. (1987), *Computation of Flow fields in Centrifugal Compressor Diffusers with Splitter Vanes*, Proc. of the International Gas Turbine Congress, 2, 311-317.
- Vavra, M. H., (1970), *Basic Elements of Advanced Design of Radial-Flow Compressors*, AGARD Lecture Series No. 89 on Advanced Compressors.
- Xu C., and R. S. Amano, (2006), *A Study of a Single Stage Centrifugal Compressor*, *ASME Electric Power Conference*, PWR2006-88023, Georgia World Congress Centre, Atlanta, GA.
- Xu C., and R. S. Amano, (2008), *Computational Analysis of Swept Compressor Rotor Blades*,” *International Journal for Computational Methods in Engineering Science and Mechanics*, 9(6), 374-382.
- Xu C., and R. S. Amano, (2009a), *Computational analysis of Scroll tongue shapes to compressor performance by using different turbulence models*. GT2007-28224.
- Xu C., and R. S. Amano, (2009b), *The Development of a Centrifugal Compressor Impeller*, *International Journal for Computational Methods in Engineering Science and Mechanics*, 10(4), 290-301.
- Xu C., and R. S. Amano, (2009c), *Development of a Low Flow Coefficient Single Stage Centrifugal Compressor*, *International Journal for Computational Methods in Engineering Science and Mechanics*, 10(4), 282-289.
- Xu, C. and R. S. Amano, (2004), *Numerical simulation of the aerodynamic effects on sweep compressor blades*, IGTI-2004-53008.
- Xu, C. and R. S. Amano, (2010), *Study of the flow in a centrifugal compressor*, *Int. J. of Fluid Machinery and System*, 3(3), 260-270.
- Xu, C. and R. S. Amano, (2012a), *Meridional considerations of the centrifugal compressor development*, *International Journal of Rotating Machinery*, 1-11.
- Xu, C. and R. S. Amano, (2012b) *Empirical Design Considerations for Industrial Centrifugal Compressors*. *International Journal of Rotating Machinery*, 1-15.
- Zangeneh, M. (1998), *On 3D Design of Centrifugal Compressor Impellers with Splitter Blades*, ASME paper 98-GT-507.